

Understanding the combination of fractional factorial design and chemometrics analysis for screening super-saturable quercetin-self nano emulsifying components

Galih Pratiwi¹, Aninditha Rachmah Ramadhiani¹, Shaum Shiyan²

¹ STIKES Aisyiyah Palembang, Palembang, Indonesia

² Universitas Sriwijaya, Indralaya, Indonesia

Corresponding author: Shaum Shiyan (shaumshiyansri@unsri.ac.id)

Received 16 January 2022 ♦ Accepted 15 February 2022 ♦ Published 5 April 2022

Citation: Pratiwi G, Ramadhiani AR, Shiyan S (2022) Understanding the combination of fractional factorial design and chemometrics analysis for screening super-saturable quercetin-self nano emulsifying components. *Pharmacia* 69(2): 273–284. <https://doi.org/10.3897/pharmacia.69.e80594>

Abstract

Quercetin is formulated in a super saturable - self-nano emulsifying (SS-SNE) to increase its stability and bioavailability. This study focuses on the screening design for SS-SNE components with a fractional factorial design (FrFD) approach and chemometric analysis. The FrFD method was chosen because it provides comprehensive benefits. The oil components used are canola and grape seed oil. Croduret 50-SS was selected as a surfactant and PEG 400 as a co-surfactant. The interaction of SNE components was evaluated using FTIR-ATR instrumentation. SNE droplet morphology was observed using a transmission electron microscope (TEM). The selected formulas were grape seed oil as oil phase at 19.6%, croduret at 60%, and PEG 400 as co-surfactant with a concentration of 16.6%. The selected formula has a droplet size of 133.27 nm, PDI of 0.181, the zeta potential of 17.00 mV, electrophoretic mobility of 1.332 $\mu\text{mcm/Vs}$, emulsification time of 10.05 seconds, a viscosity of 370.147 mPa.s, and a drug load of 31.70 mg/mL. The components of grape seed oil, croduret, and PEG 400 resulted in a quercetin carrier SNE formula that met the criteria. FrFD design and chemometric analysis in the screening process can help determine the selected formula very effectively and efficiently.

Keywords

chemometrics, cluster analysis, design of experiment, fractional factorial design, nanoemulsion, principal component analysis, quercetine, SNE

Introduction

Quercetin has the basic structure of flavonols, one of the six sub-class of flavonoid compounds. Quercetin or 3,3',4',5,7-pentahydroxyflavanone has pharmacological activities as an antidiabetic (Srinivasan et al. 2018), anti-inflammatory (Cheng et al. 2019), anticancer (Li et al. 2018; Tang et al. 2020) and antivirals (Ferreira et al. 2018).

Quercetin, as an aglycone form of flavonoids, has low bioavailability and poor pharmaceutical stability. The low bioavailability of quercetin is due to its low water solubility (Dwi et al. 2018). Therefore, we need a breakthrough in the formulation of delivery system with a more effective and efficient approach.

Self-nano emulsifying drug delivery system (SNEDDS) has been developed to form emulsions with nanometer

size to increase oral bioavailability (Anwer et al. 2021). The modified self-nano emulsifying (SNE) formulation was chosen because it is more stable than nanoemulsion containing water and has a minimal volume (Altamimi et al. 2019; Cardona et al. 2021; Shiyani et al. 2022). Super saturable-SNE is an SNE system containing a water-soluble polymer precipitation inhibitor that can produce and maintain a metastable drug in a saturated state in the gastrointestinal tract. The aim is to prevent the tendency of SNE to precipitate when diluted in gastric media, which results in reduced in vitro dissolution and in vivo absorption (Zhang et al. 2020). The SNE formulation consists of oil, surfactants, and co-surfactants that form emulsions spontaneously and rapidly when they meet water (Halder et al. 2021; Shiyani et al. 2021). Oil components used as drug carriers in the SNE system are grape seed oil and canola oil. Croduret 50-SS is used as a surfactant that can reduce oil and water interface tension. Polyethylene glycol (PEG 400) as a co-surfactant helps the surfactant maintain the stability of the film layer between oil and water (Ogino et al. 2021). Croduret 50-SS and PEG 400 have a hydrophilic-lipophilic balance (HLB) value of more than ten and meet SNE formulation requirements. The higher HLB makes the formation of nanoemulsion easier.

The SNE formulation can increase the solubility of active substances and increase transport through the intestinal lymphatic system. That strategy can avoid *P*-glycoprotein release to increase absorption and bioavailability (Dhritlahre et al. 2021). The success of SNE formulating lipid-based drug carriers depends on the type of oil, surfactant, and concentration ratio of each component (Shiyani et al. 2021). The solubility of active drug substance in each type of oil, surfactant, and co-surfactant resulted in different SNE characteristics. The observed characteristics are droplet size, polydispersity index (PDI), zeta potential, mobility, emulsification time, viscosity, and loading drug. The selection of constituent components such as oil, surfactant, and co-surfactant is an essential factor for formulating SNE with characteristics that meet the requirements.

The screening stage for both nanoemulsion and SNE formulations is done manually or semi-designed using pseudo ternary diagrams (Puppala and Lakshmi 2019). However, pseudo ternary use still requires a large number of trials and cannot predict the optimum conditions effectively (Ahmad et al. 2013). This approach is different from the application of the design of experiment (DoE). Evaluation using the DoE application with the fractional factorial design (FrFD) method will provide a more advantage at the screening stage. This method is carried out simultaneously and comprehensively compared to trial and error using a large number of samples. The resulting SNE characteristics provide qualitative information and quantitative effects, using the DoE mathematical modeling approach, with the FrFD method. The use of FrFD is also more effective and efficient because it uses a small number of samples.

The FrFD approach with mathematical modeling can provide qualitative information and quantitative influence on the characteristics of the formula. However, the analysis on the run of the FrFD design could not obtain information about grouping based on the formula's characteristics and the correlation between responses. This information is critical in evaluating the response to further optimization procedures. Therefore, it is a novelty in the FrFD analysis combined with the chemometric approach. FrFD evaluation can be combined with chemometric analysis using principal component analysis (PCA) and cluster analysis (CA) techniques. The factors observed were grape seed oil and canola oil components linked to croduret 50-SS and PEG-400. The responses observed as parameters were droplet size, PDI, zeta potential, mobility, emulsification time, viscosity, and drug load. It is hoped that in the future, SSQ-SNE formulations can improve the quercetin delivery system.

Materials and methods

Chemicals and materials

Quercetin was purchased from Sigma-Aldrich. Grape seed oil under the Aceites Borges brand name and Palmtop canola oil is obtained from a local Palembang supermarket. Croduret 50-SS from Croda, PEG-400, and aquadest were purchased from Bratachem.

Preparation of super saturable quercetin - self-nano emulsifying (SSQ-SNE)

SNE was prepared by dissolving quercetin with carrier oil using vortex followed by ultrasonication for 5 minutes at room temperature. Surfactants and co-surfactants are added to the oil-quercetin solution. The homogeneous mixture was placed in a rotary shaker (25–30 °C for 12 hours) and allowed to stand again for 12 hours (Ogino et al. 2021; Shiyani et al. 2022).

Design of experiment for screening component SSQ-SNE

The experimental design for screening the constituent components of SNE was carried out using the FrFD 2^{4-1} approach. The formulation design was determined by factors including the type of oil (A; canola oil and grape seed oil), the concentration of surfactants (B; %), the concentration of co-surfactants (C; %), and oil concentration (D; %). The FrFD approach uses two levels (upper limit +1 and lower limit -1) in a certain portion. The category choice is used for A and numeric factors for B, C, and D in preparing the formula design. Canola and grape seed oil use a lower limit of 14% and an upper limit of 20%, respectively. The croduret concentration range uses a lower limit of 30% and an upper limit of 60%. Co-surfactant PEG 400 uses a lower limit range

Table 1. Design and complete experimental results of the FrFD 2⁴⁺¹.

Run	SNEDDS components				Responses (R _n)						
	A	B	C	D	R ₁	R ₂	R ₃	R ₄	R ₅	R ₆	R ₇
1	Canola	60	30	20	26.88 ± 1.33	0.406 ± 0.005	25.27 ± 1.32	2.210 ± 0.10	10.07 ± 0.15	668.01 ± 19.13	17.41 ± 0.78
2	Grape seed	60	30	14	43.12 ± 2.07	0.345 ± 0.009	28.40 ± 0.89	2.186 ± 0.02	12.43 ± 0.15	676.49 ± 34.58	25.94 ± 1.04
3	Grape seed	60	10	20	130.07 ± 7.41	0.534 ± 0.016	23.10 ± 1.51	1.812 ± 0.12	8.60 ± 0.10	283.49 ± 9.04	29.01 ± 1.26
4	Canola	30	10	20	146.47 ± 13.86	0.510 ± 0.023	21.67 ± 0.57	1.728 ± 0.03	28.93 ± 1.42	942.27 ± 94.73	46.79 ± 0.96
5	Canola	60	10	14	266.53 ± 12.01	0.408 ± 0.034	23.47 ± 1.05	1.705 ± 0.02	19.37 ± 0.38	1216.73 ± 70.98	33.86 ± 2.16
6	Grape seed	30	30	20	164.00 ± 0.79	0.391 ± 0.027	23.70 ± 0.53	1.862 ± 0.04	9.67 ± 0.55	946.63 ± 101.29	35.28 ± 2.04
7	Canola	30	30	14	26.74 ± 0.51	0.330 ± 0.012	19.13 ± 0.85	1.376 ± 0.07	11.47 ± 1.21	851.85 ± 21.84	28.72 ± 0.89
8	Grape seed	30	10	14	121.10 ± 5.12	0.528 ± 0.032	16.64 ± 0.35	1.336 ± 0.06	19.47 ± 0.55	786.09 ± 25.35	42.69 ± 1.73

Note: (A) Oil type, (B) Surfactant concentration (%), (C) Co-surfactant concentration (%), (D) Oil concentration (%), (R₁) Droplet size, (R₂) Polydispersity index, (R₃) Zeta potential, (R₄) Electrophoretic mobility, (R₅) Emulsification time, (R₆) Viscosity, (R₇) Drug load.

of 10% and an upper limit of 30%. The main responses observed and measured consisted of droplet size (R₁; d.nm), polydispersity index (R₂), zeta potential (R₃; mV), electrophoretic mobility (R₄; μmcm/Vs), emulsification time (R₅; seconds), viscosity (R₆; mPa.s) and drug load (R₇; mg/mL). The complete design and data of the eight experiment runs are shown in Table 1.

Chemometrics analysis for study at run formula

The data obtained were also analyzed using a chemometric approach with the PCA and CA methods. The PCA-CA method was processed using Minitab 17 series software (Minitab, State College, PA, USA). Evaluation at this stage is not part of modeling and prediction optimization, but evaluation of 8 runs and the correlation between responses (Kartini et al. 2020; Shiyani et al. 2021).

Droplet size, polydispersity index, zeta potential, and mobility

The optimum droplet diameter, polydispersity index (PDI), and zeta potential of SSQ-SNE formula were measured using a particle size analyzer Zetasizer Nano ZSP (Malvern Panalytical, UK) by applying the dynamic light scattering (DLS-PSA) method. Data was collected in triplo ($n=3$) and presented in the form of mean ± standard deviation. The data processing used Zetasizer 7.12 (Malvern Panalytical) software which helped the analysis run, in order to obtain results in the form of particle size (d.nm), PDI, zeta potential (mV) and electrophoretic mobility (μmcm/Vs).

Measurement of emulsification time, viscosity, and drug load

Emulsification is essentially the process of dispersing SSQ-SNE in aqueous media to form a nanoemulsion. A total of 1 mL of SSQ-SNE is dropped into 500 mL of media. The dispersing process is conditioned at 37 °C on the magnetic stirrer with a stirring rate of 120 rpm. Observations were made on time it took from the start of the drop until the nanoemulsion was formed. Visual

observations were made by looking at the nanoemulsion efficiency, transparency, phase separation, and quercetin droplets. The nanoemulsion formed was characterized by the complete dissolution of SSQ-SNE in the medium (Shiyani et al. 2021). SSQ-SNE viscosity measurement uses an Oswald viscometer in mPa.s units (Yadav et al. 2014). The quantity of quercetin contained in SNE was measured by centrifugation at 3500 rpm for 30 minutes. The precipitate formed is weighed as quercetin, which does not enter the system.

Percentage of clarity studies

A total of 100 μL of SSQ-SNE was emulsified into 10 mL of aqua pro injection. Clarity (transmittance; %) was determined using a Genesys 10S UV-Vis spectrophotometer (Thermo Scientific, USA) at a wavelength of 650 nm and the blank solution is purified water.

Thermodynamic stability studies

Stability tests for SSQ-SNE and nanoemulsions using heating-cooling and freezing methods in selected formulas. Centrifugation studies were carried out at 3500 rpm for 30 minutes, and visual observations were made to confirm phase separation, precipitation, instability, cracking, or cream formation (Jumaryatno et al. 2018).

Morphology characterization and interaction studies

The morphology of nanoemulsion globules or droplets was identified using a transmission electron microscope (TEM). The TEM instrumentation used was JEM 2100 (Jeol, Tokyo, Japan). The interaction of SNE constituent components was identified using Fourier transform infrared spectrophotometry-attenuated total reflectance (FTIR-ATR) Nicolet iS5 (Thermo Scientific, USA). Spectra readings were carried out on SSQ-SNE, quercetin material, oil (canola and grape seed), surfactant (croduret 50-SS), and co-surfactant (PEG 400). IR spectra readings were carried out at a wavenumber between 4000 cm⁻¹ to 500 cm⁻¹.

Result and discussion

Fractional factorial design for screening component SSQ-SNE

The FrFD approach to screening provides a more effective and efficient measure. Statistical data from the fitting model on all evaluated responses are presented in Table 3. The droplet size model has an R^2 value of more than 0.7, with an adjusted R^2 value of 0.9985. Predicted R^2 is 0.9929, and the difference between adjusted R^2 and predicted R^2 is less than 0.2. The value of adequate precision reinforces the model if the value is more than 4. The polydispersity index also shows an adequate response in modeling. The fitting model is included in the right criteria for predicting the selected or optimal formula by considering the value of R^2 , adjusted R^2 , predicted R^2 , adequate precision, and press (Pratiwi et al. 2019; Shiyani et al. 2019).

Zeta potential is an essential parameter in determining the best formula for SSQ-SNE. The results of the fitting of the model for zeta potential, R^2 value 0.9837, adjusted R^2 0.9428, predicted R^2 0.7385, and adequate precision 15.72. Overall, the statistical evaluation of each parameter or response is very suitable for use in prediction. Based on the fitting model results, all responses have the same model, namely reduced 2FI. Based on ANOVA analysis, the equation and model for the response to droplet size

(R_1) showed significant results $p < 0.05$. Each of the SNE constituent components, namely the type of oil (A), the concentration of croduret (B), the concentration of PEG-400 (C), and the concentration of oil (D), affect the increase in the size of the resulting droplets. The type of oil (A) and the interaction between the type of oil and the concentration of Croduret as a surfactant (AB) can increase the droplet size diameter. Oil as a carrier will interact and dissolve the active substance in a certain amount so that the interaction of oil with surfactants will increase the droplet size. The concentration of PEG as co-surfactant (C), the interaction of oil type with PEG concentration (AC), and type of oil with oil concentration (AD) can reduce droplet size.

The effect of the SNE components on droplet size was evidenced from the experimental results (Table 1) and evaluation of the FrFD-chemometric combination. Experiments on the eight runs resulted in varying diameters from 26.74 ± 0.51 nm to 266.53 ± 12.01 nm. Large droplet size is strongly influenced by the interaction of the type of oil and croduret as a surfactant. The relationship between the response (R_1) and the independent variables or factors (A, B, C, and D) can be seen in the 3D surface plot of Fig. 2A. The appearance of SSQ-SNE and nanoemulsion from eight trial runs is presented in Table 2 and Fig. 1. The effect of the PDI nanoemulsion response components can be seen in equation 4 (Table 4). The dominant factors that influence the PDI value are the type of oil (A), PEG-400 concentration (C), and oil concentration (D), AC interaction, and AD interaction. The components of the factors mentioned above can affect the PDI of the resulting nanoemulsion. Based on ANOVA analysis, the p -value is less than 0.05, indicating a significant model.

Type of oil (A), the concentration of croduret (B), the concentration of PEG-400 (C), and concentration of oil (D) affect the increase in electrophoretic mobility of the resulting SNE. Electrophoretic mobility can be decreased by the interaction of oil types with PEG-400 (AC) concentrations. The emulsification time can be decreased by the interaction of oil type with PEG-400 (AC) concentration. The interaction of oil type with oil concentration (AD) increases the emulsification time. The interaction between the type of oil and the concentration of croduret (AB) causes an increase in viscosity. The interaction between types of oil

Table 2. Visual observation of SNEDDS and formed nanoemulsion.

Run	Visual SNEDDS	SNEDDS color	Precipitation on SNEDDS	Clarity (% T)	
				SNEDDS	Nanoemulsion
1	No separation	Clear yellow	No	75.35 ± 1.33	98.67 ± 0.60
2	No separation	Clear yellow	No	71.97 ± 0.63	99.99 ± 0.01
3	No separation	Clear yellow	No	62.06 ± 1.24	98.63 ± 0.58
4	No separation	Tawny	No	49.37 ± 1.47	44.42 ± 0.59
5	No separation	Clear yellow	No	64.52 ± 1.17	99.54 ± 0.51
6	No separation	Tawny	No	54.04 ± 0.49	75.62 ± 0.61
7	No separation	Tawny	No	66.67 ± 0.68	99.67 ± 0.51
8	No separation	Tawny	No	52.44 ± 0.96	99.66 ± 0.57

Note: The transmittance nanoemulsion was measured from the SNEDDS emulsification results with a dilution of 500 times.

Table 3. Statistical parameters for the overall response of the FrFD.

Response	Parameter							
	Standar deviasi	Mean	CV (%)	Press	R^2	Adjusted R^2	Predicted R^2	Adequate precision
R_1	3.23	115.61	2.80	334.39	0.9996	0.9985	0.9929	86.49
R_2	0.02	0.432	3.95	0.01	0.9876	0.9565	0.8013	14.95
R_3	0.86	22.67	3.81	23.89	0.9837	0.9428	0.7385	15.72
R_4	0.04	1.78	2.49	0.06	0.9946	0.9812	0.9140	24.00
R_5	1.54	15.00	10.29	76.20	0.9862	0.9518	0.7797	15.21
R_6	60.38	796.45	116700	0.99	0.9859	0.9507	0.7746	17.85
R_7	0.74	32.46	2.29	17.73	0.9982	0.9937	0.9712	45.10

Note: (R_1) Droplet size, (R_2) Polydispersity index, (R_3) Zeta potential, (R_4) Electrophoretic mobility, (R_5) Emulsification time, (R_6) Viscosity, (R_7) Drug load.

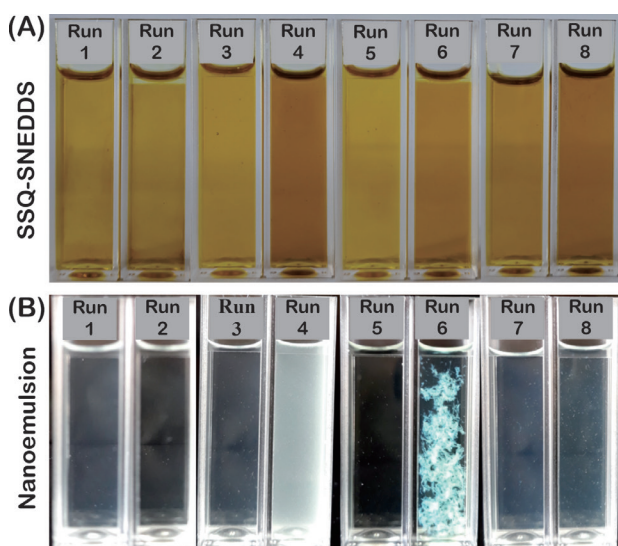


Figure 1. Visual appearance of SSQ-SNE and nanoemulsion of eight FrFD 2^{+1} runs, (A) SNE, (B) nanoemulsion.

with a concentration of PEG-400 (AC) can reduce viscosity. Drug load is strongly influenced by the type of oil (A) and the concentration of PEG 400 (C).

The interaction of oil types with Croduret and PEG-400 for each response is shown in Fig. 3. The use of croduret with high grape seed oil concentrations will produce small-

er droplet sizes than interactions with canola oil (Fig. 3A). The PDI was smaller when the PEG-400 concentration was higher, whether the interaction was in grape seed or canola oil. The lower PEG-400 concentration gave a greater PDI, especially its interaction with grape seed oil. The increase in the croduret concentration could increase the zeta potential, interacting with grape seed oil and canola oil (Fig. 3C). The interaction between grape seed oil and the higher PEG-400 concentration increased the level of electrophoretic mobility. However, the interaction of canola oil and high concentrations of PEG-400 resulted in lower mobility (Fig. 3D). The emulsification time will be longer at the interaction of low concentration PEG-400 with canola oil, while the interaction with grapeseed oil still results in a faster emulsification time (Fig. 3E). The interaction between canola oil and high concentrations of croduret resulted in a high SNE viscosity (Fig. 3F). A high drug load was obtained at canola oil interaction with low concentrations of PEG-400 (Fig. 3G).

Principal component analysis and cluster analysis on the FrFD

The response data from the SSQ-SNE formulas that have been obtained were analyzed using a chemometric approach with the principal component analysis (PCA) and cluster analysis (CA) methods. The multivariate approach using

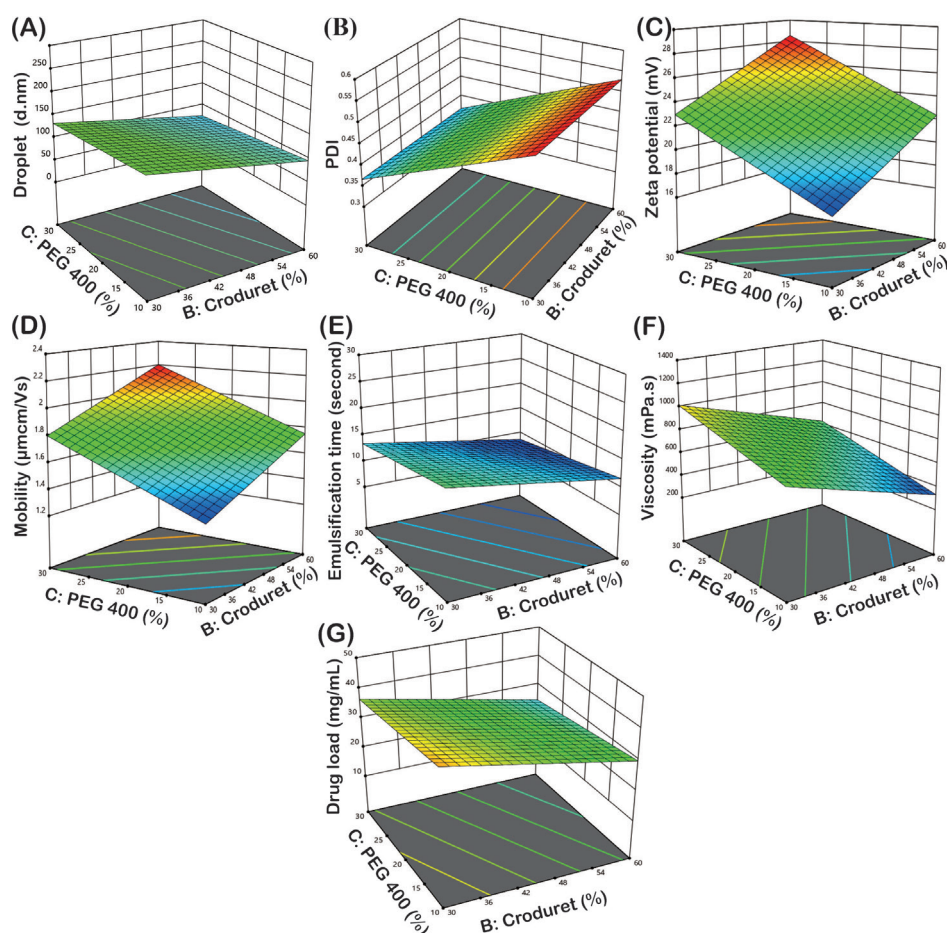


Figure 2. Graph of the 3D model surface plot of the evaluated responses, (A) droplet size (B) Polydispersity index, (C) zeta potential, (D) electrophoretic mobility, (E) emulsification time, (F) viscosity, (G) drug load.

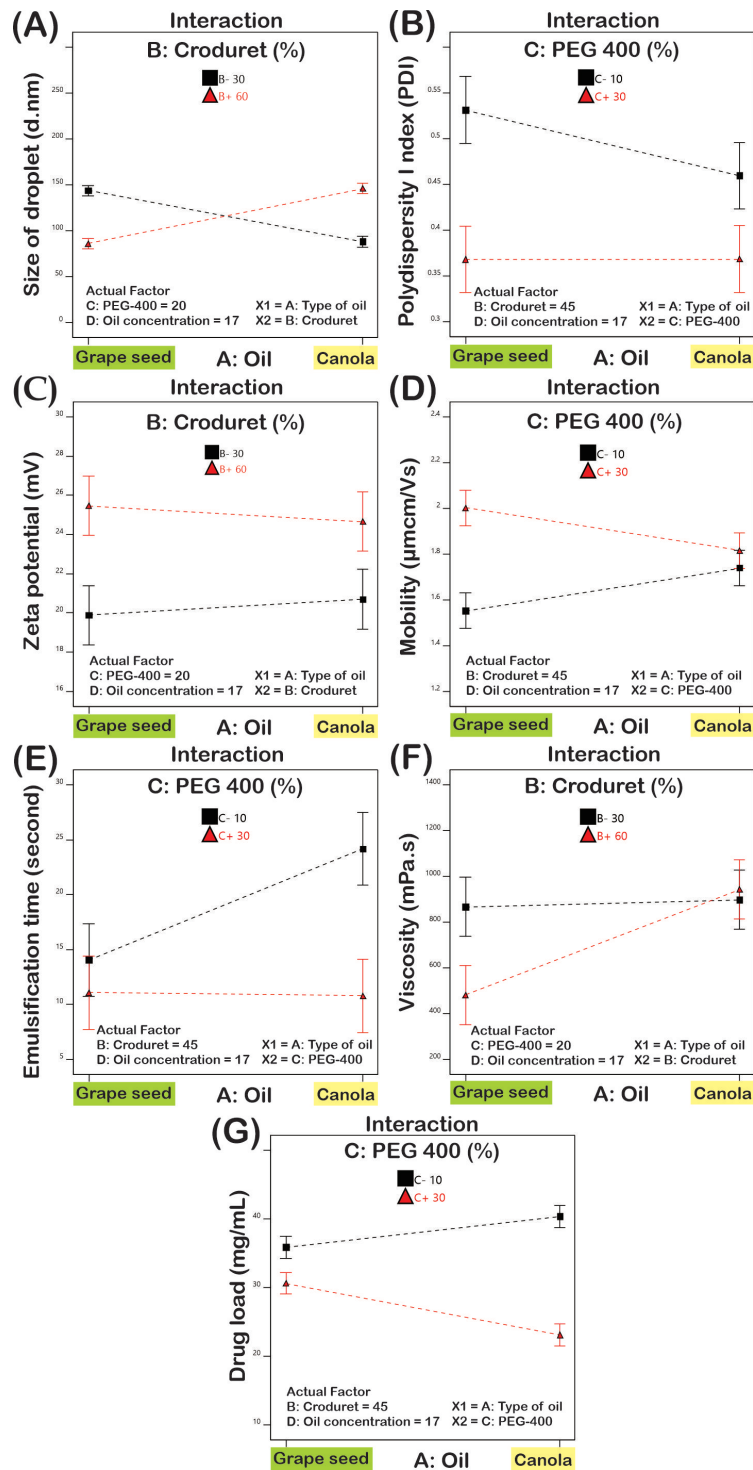


Figure 3. Graph of interactions between factors on the evaluated response, (A) droplet size (B) Polydispersity index, (C) zeta potential, (D) electrophoretic mobility, (E) time of emulsification, (F) viscosity, (G) drug load.

PCA aims to simplify variables by reducing data from a large number of interrelated variables without changing existing information (Cui et al. 2021; Shiyan et al. 2021; Kim et al. 2022). CA technique is a method based only on information found in data that describes relationships and objects or is based on similar characteristics of these objects. CA analysis forms and separates groups with the closest relationship in more detail to provide more accurate information (Iaboni et al. 2020; García del Moral et al. 2021).

Fig. 4B is a score plot that shows the run formula grouping into 5 clusters. The score plot classifies the samples based on the run composition function and the resulting response (Talekar et al. 2019; Hong et al. 2021). Multivariate analysis was successful in grouping the runs at different distances from each other. The distance between runs or samples shows the similarity of characteristics. The further distance between the runs indicates little similarity in traits or characteristics (Shiyan et al. 2020; Setyawan

Table 4. The type of model and the equation of each response.

Response	Model	Regression equation
R ₁	Reduced 2FI	$R_1 = 1.04A - 50.43C + 29.02AB - 39.42 AC - 31.22AD \dots\dots(1)$
R ₂	Reduced 2FI	$R_2 = 0.02A - 0.06C + 0.03D + 0.02AC + 0.02AD \dots\dots\dots(2)$
R ₃	Reduced 2FI	$R_3 = 2.39B + 1.45C + 0.76D + 0.40AB - 1.64AC \dots\dots\dots(3)$
R ₄	Reduced 2FI	$R_4 = 0.20B + 0.13C + 0.13D - 0.76AC + 0.09AD \dots\dots\dots(4)$
R ₅	Reduced 2FI	$R_5 = 2.46A - 2.38B - 4.09C - 2.60AC + 2.72AD \dots\dots\dots(5)$
R ₆	Reduced 2FI	$R_6 = 123.27A - 85.27B - 86.34D + 107.92B - 149.08AC \dots\dots\dots(6)$
R ₇	Reduced 2FI	$R_7 = 0.77A - 5.91B - 5.63C - 3.00AC + 0.74AD \dots\dots\dots(7)$

Note: (A) Oil type, (B) surfactant concentration (%), (C) co-surfactant concentration (%), (D) oil concentration (%), (R₁) Droplet size, (R₂) Polydispersity index, (R₃) Zeta potential, (R₄) Electrophoretic mobility, (R₅) Emulsification time, (R₆) Viscosity, (R₇) Drug load.

et al. 2021). The dendrogram in CA can group the same variables and have bonds in one group based on the value of closeness (similarity) (Szentmiklóssy et al. 2020). The characteristic similarity index is depicted in dendrogram form in Fig. 4C. Each run is classified based on its similarity. Run 1 and 2 have a closeness with a value of 97.82%; run 4 and 6 have a closeness of 96.94%; 7 and 8 have a value of 85.56%. The proximity of each run was also evidenced by a similar FTIR-ATR spectra pattern (Fig. 6A).

The loading plot aims to determine the variable of a sample or formula that most contributes to forming the principal component (PC) values. The contribution of the sample variables to the loading plot can be seen from a distance used. Data analysis using the PCA loading plot depicts the angle that shows a correlation between the responses of all formulas. The responses of R₃ and R₄, which form an adjacent angle (less than 45°), indicate a positive correlation. The electrophoretic mobility (R₄) of the droplets will increase with the high zeta potential (R₃) value. A negative correlation occurs between R₂ and R₃, which forms an angle close to 180°. A high polydispersity index (R₂) can reduce the zeta potential (R₃). The angle between the two vectors that are close to 90° indicates no correlation between responses.

Selected formulas and verification of results

The best formula for screening can be predicted by the model obtained from the FrFD. The most critical stage in prediction is to determine the level of importance and goals of each response. The target droplet size is 50 nm, with an important level value of 5. The polydispersity index has a lower limit of 0.33 and an upper limit of 0.54 with an in-range target and an important level value of 3. Zeta potential in the FrFD²⁺¹ experiment produces a range of 16.64–28.40 mV. Considering this response is related to stability, the prediction stage uses a target of 25 mV and the value of importance 4. Electrophoretic mobility in the

in-range target with a level of importance of 3 is positively correlated with zeta potential. The emulsification time and viscosity were determined with minimum targets with importance values of 5 and 4. Considering the super saturable-SNE formulated, the target set for drug load must be a maximum with a level of importance of 4.

The SNE components selected were grape seed as the oil phase, croduret as a surfactant, and PEG-400 as a co-surfactant with concentrations of 19.6%, 60%, and 16.6%, respectively. The desirability value is an essential indicator in determining the selected formula mixture in the SSQ-SNE formulation. The desirability at the prediction stage obtained a value of 0.751. High desirability values (close to 1) indicate the ability of the FrFD design to produce perfect predictions and proper screening procedures (Shiyan et al. 2019; Indrati et al. 2020). The desirability value provides an overview of the similarity between the predicted value and the actual observation. The composition of SSQ-SNE selected in FrFD 2⁺¹ obtained optimum results with a droplet size of 112.84 d.nm, a polydispersity index of 0.487, a zeta potential of 25 mV, mobility of 1.932 μmcm/Vs, an emulsification time of 8.60 seconds, a viscosity of 364.72 mPa.s, and drug load of 27.64 mg/mL.

Characterization and evaluation of selected SSQ-SNE

Appearance, drug load, and viscosity

The visuals observed include color, odor, separation, and precipitation. SSQ-SNE is yellowish, clear, slightly thick due to the addition of surfactant and a slightly pungent odor of oil. The yellow color of SNE is affected by quercetin (Fig. 5C). In general, drug load is used to determine drug solubility in SNE components (Indrati et al. 2020). The drug load parameter in this study indicated the level of quercetin saturation in the SNE system. The selected formula in the saturated state had a drug load of 31.70 ± 1.15 mg/mL.

Viscosity on SNE will affect the ease of use and the formation of nanoemulsion droplets. The low viscosity is due to the smaller globule size of oil (Anwer et al. 2021). The SNE form, which resembles a gel character, has a high viscosity so that after contact with water, it produces a relatively longer dispersion (emulsification time runs slowly). In contrast, low viscosity (which does not resemble a gel) will emulsify more easily. The SSQ-SNE viscosity in the selected formula is 370.15 ± 7.69 mPa.s, still has suitable viscosity with emulsification time of fewer than 5 minutes.

Emulsification time

Emulsification time describes the length of time to produce nanoemulsion from SNE when it encounters gastrointestinal fluids. The selected formula showed an emulsification time of fewer than 5 minutes in a medium of 10.05 ± 0.33 seconds. The faster the SNE turns into nanometer-sized droplets, the faster the drug will dissolve and be absorbed into the blood vessels (Dhritlahre et

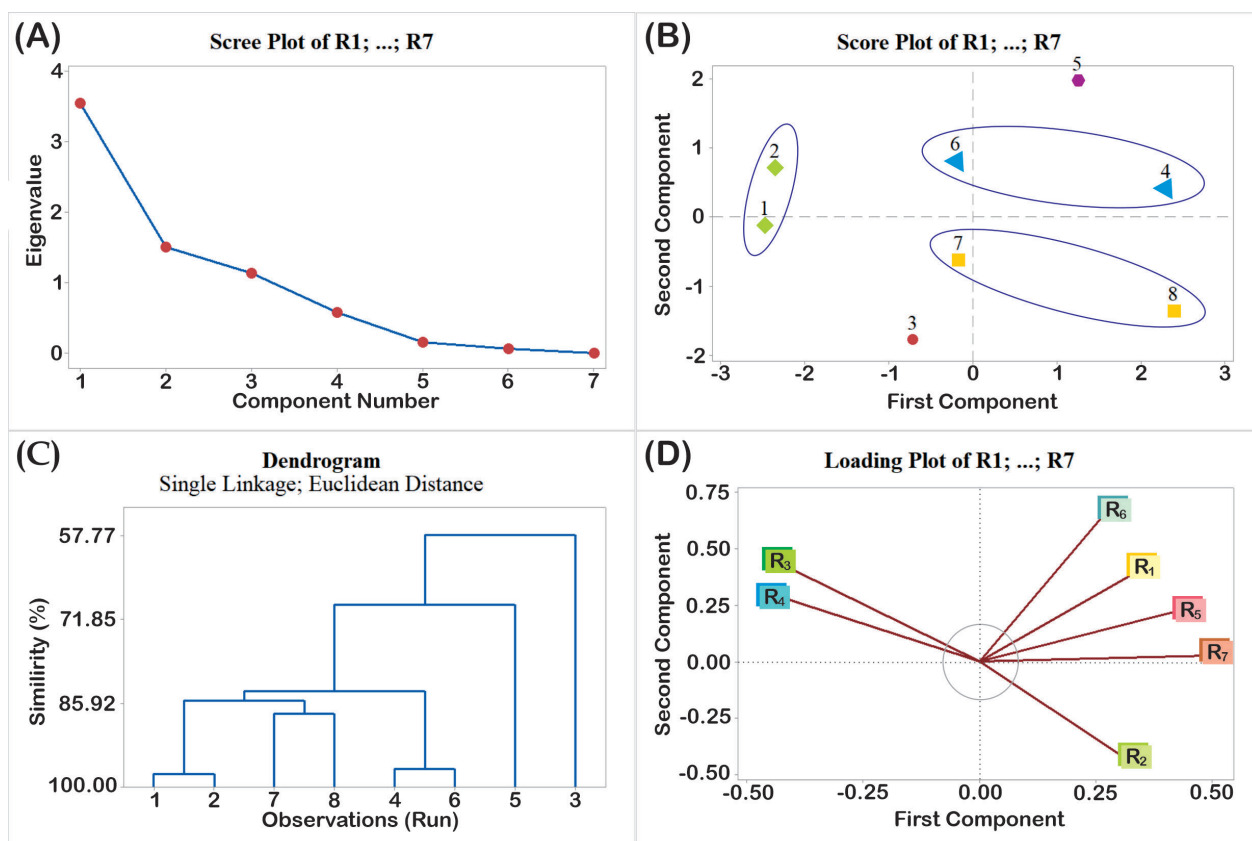


Figure 4. The results of a chemometric analysis using the PCA-CA approach, (A) scree plot, (B) score plot, (C) dendrogram, (E) loading plot.

al. 2021; Jumaryatno et al. 2018). Emulsification rate is positively correlated with viscosity, referring to the loading plot (Fig. 4D) of vectors R₅ and R₆ forming an angle of less than 45°. SNE with high viscosity will spread slowly or emulsify slowly, while SNE with low viscosity will emulsify more easily.

Morphology, droplet size, and polydispersity index

The instrument used to determine droplet morphology was transmission electron microscopy (TEM). The observations show that the form of nanoemulsion particles produced is spherical (Fig. 5A, B). Droplet size is a crucial characteristic in assessing a good nanoemulsion. The selected formula has a droplet diameter of 133.27 ± 0.64 nm. The droplet size is calculated from the volume, intensity, and bimodal distribution, assuming spherical particles. Droplet size is an essential factor in the SNE formulation, as it determines the rate of drug release, absorption, and increases bioavailability (Anwer et al. 2021; Cardona et al. 2021). The droplet diameter also depends on the type of oil phase formulated because it affects the formation of oil globules (Indrati et al. 2020). Discussing nanoemulsion not only focuses on droplet size but also the polydispersity index (PDI), which provides information on size homogeneity (Shiyan et al. 2022). Theoretically, the higher the PDI value, the lower the uniformity of globule size from nanoemulsion. PDI is the standard

deviation value from the mean particle size used as the uniformity parameter for the nanoemulsion evaluation. The polydispersity index value is getting below 1, indicating the uniformity of the nanoemulsion size formed. The measurement results in the selected formula, the PDI value is 0.181 ± 0.01 .

Zeta potential and electrophoretic mobility

The zeta potential describes the repulsion between the droplets. The strength of the attraction or repulsion is determined by hydrogen bonds and van der Waals bonds. The zeta potential value away from zero will be more stable because it minimizes aggregation. Zeta potential as the main parameter can describe the stability of nanoemulsion. The droplet in the selected formula has a zeta potential value of 25.03 ± 2.53 mV with a negative charge (Fig. 5G). The negative charge is caused by the presence of free fatty acids in the formula (Balakumar et al. 2013). The zeta potential value that is ahead of zero theoretically shows a more stable nanoemulsion. In addition to the zeta potential, the electrophoretic mobility clarifies the study of nanoemulsion stability. This parameter describes the velocity of the droplet. The higher the zeta potential value, both positive and negative charges, the higher the electrophoretic mobility value (Pratiwi et al. 2019). The electrophoretic mobility on the selected SSQ-SNE was 1.332 ± 0.19 $\mu\text{mcm/Vs}$.

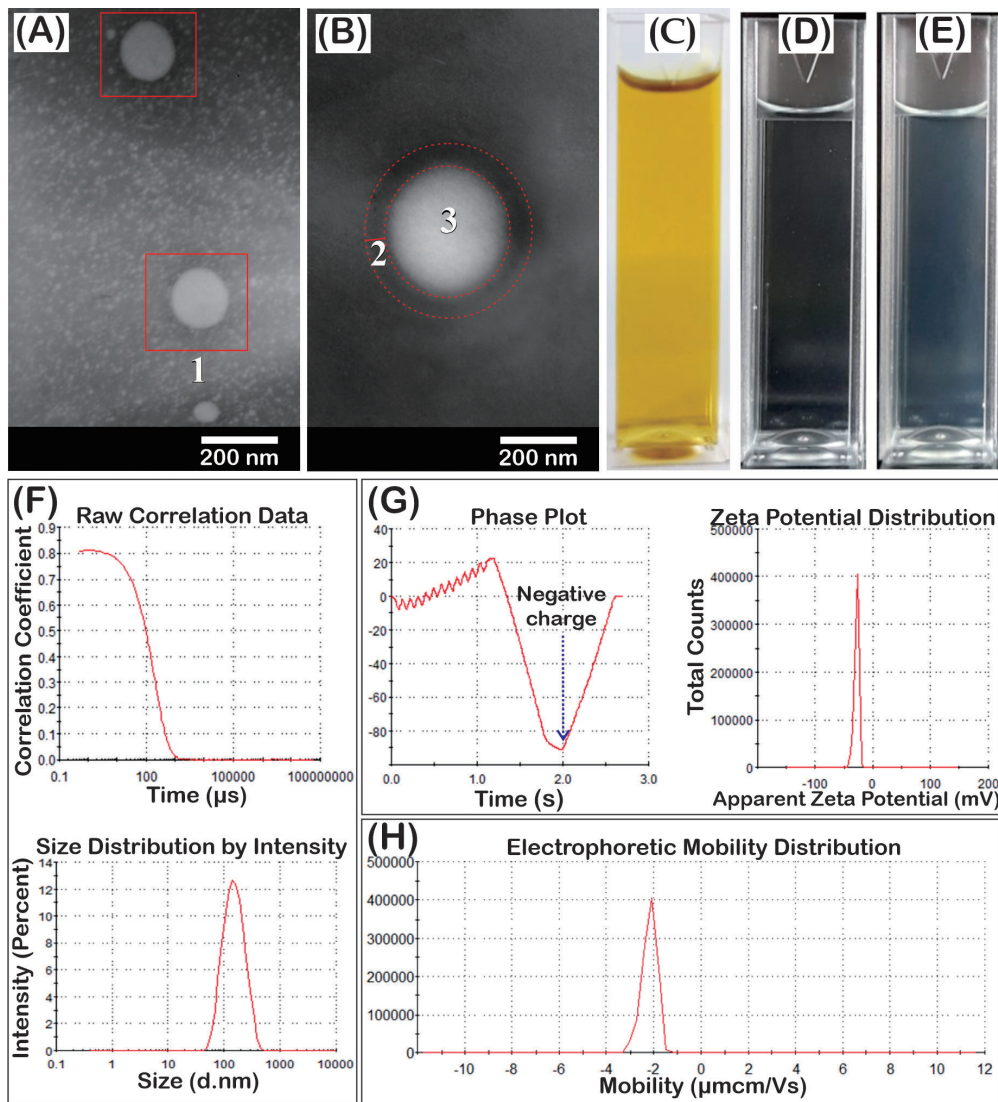


Figure 5. SSQ-SNE characterization using selected formulas, (A) droplet morphology from TEM, (B) droplets with oil and surfactant globules, (C) SNE, (D) nanoemulsion with 500 times dilution, (E) nanoemulsion with 100 times dilution, (F) droplet size measurement results using DLS-PSA, (G) zeta potential with a negative charge, (H) electrophoretic mobility measurement results, (I) droplet, (2) surfactant and co-surfactant area, (3) oil and quercetin.

Analysis of SSQ-SNE components using FTIR-ATR

The interaction analysis of constituent materials used FTIR instrumentation based on vibrations in each SNE component (Pratiwi et al. 2020; Shiyani et al. 2022). The spectral patterns on the SNE constituent components of quercetin, canola oil, grapeseed oil, croduret 50-SS, and PEG-400 are presented in Fig. 6. The spectral patterns of the eight runs on FrFD at first glance look similar, but in a more detailed evaluation, the intensity at the peak is different. SNE has a typical peak at wavenumbers 3300–3600 cm^{-1} , 2800–3500 cm^{-1} , 2200–2400 cm^{-1} , and a fingerprint area of 500–1800 cm^{-1} . The spectral pattern of the selected SSQ-SNE can be observed in Fig. 6B with the ratio of the components used. Quercetin spectra (Fig. 6B) have typical peaks that widen in 3000–3600 cm^{-1} . The

peak was lost in the SSQ-SNE spectra (Fig. 6B). Based on the FTIR-ATR spectra pattern and droplet morphology of TEM, quercetin was successfully incorporated into the oil globule system (SNE). Theoretically, verification is carried out by evaluating changes of spectral patterns in each component and the SNE.

Thermodynamic stability of SSQ-SNE and nanoemulsions

Physical stability is carried out to determine the maximum storage time leading to separation of the emulsion phase (creaming or cracking). Heating cooling was chosen as an accelerated thermodynamic stability test method because, with a short time, the kinetic stability of SNE could be known through the phase separation that occurred. Observations on the stability of SNE and

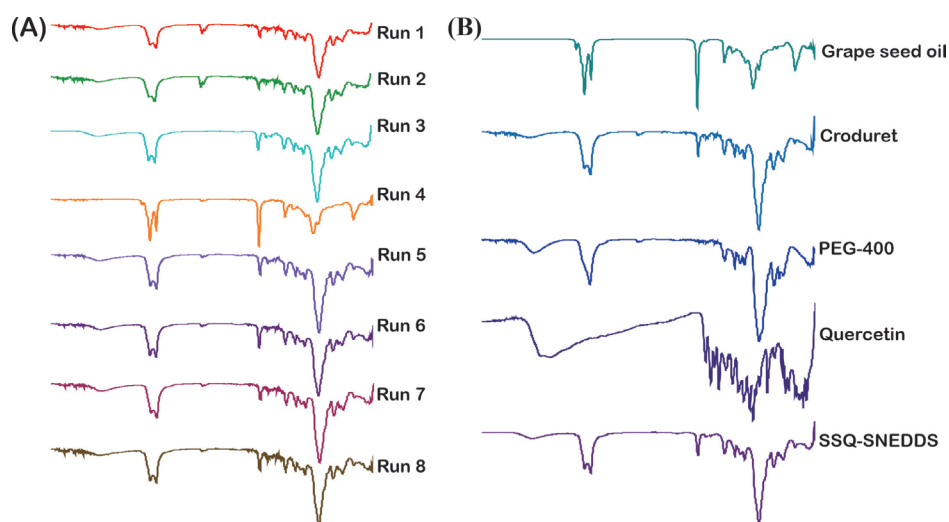


Figure 6. Profile of FTIR-ATR spectra, (A) overlay spectra of eight runs on FrFD, (B) SSQ-SNE using selected formulas and constituent components.

Table 5. The SSQ-SNE and nanoemulsion stability test.

Parameters	SSQ-SNE			Nanoemulsion		
	Stability	Color	Clarity (%T)*	Stability	Color	Clarity (%T)*
Before test	–	Clear yellow	98.45 ± 0.84	–	Clear	99.87 ± 0.16
Centrifugation	Stable	Clear yellow	98.69 ± 1.65	Stable	Clear	98.90 ± 0.45
Heating-Cooling	No separation	Clear yellow	95.53 ± 1.06	No separation	Clear	98.46 ± 1.14
Freeze-Thaw	No separation	Clear yellow	95.72 ± 1.10	No separation	Clear	98.85 ± 0.97

nanoemulsions were carried out visually to see their clarity, physical changes such as creaming, cracking, and the formation of deposits. The stability testing results using the heating-cooling and free-thaw method showed that the selected SNE and nanoemulsion formulas remained stable (Table 5). SNE and nanoemulsions show no phase separation (Fig. 5C–E).

Conclusion

The FrFD design and chemometric analysis in the screening process of the SSQ-SNE formulation have proven to be effective and efficient. SSQ-SNE comprises grape seed oil, croduret, and PEG 400 to produce a formula that meets the criteria. Screening results can be continued at the optimization stage with more comprehensive factors and responses. The formula developed is following the target in increasing the solubility and bioavailability of quercetin.

References

- Ahmad J, Amin S, Kohli K, Mir SR (2013) Construction of pseudoternary phase diagram and its evaluation: Development of self-dispersible oral formulation. *International Journal of Drug Development & Research* 5(2): 84–90.
- Altamimi MA, Kazi M, Hadi Albgori M, Ahad A, Raish M (2019) Development and optimization of self-nanoemulsifying drug delivery

Funding

This study was supported by Direktorat Riset dan Pengabdian Masyarakat Direktorat Jendral Riset dan Pengembangan Kementerian Riset, Teknologi dan Pendidikan Tinggi with contract number 849/SP2H/LT/MONO/LL2/2020, in accordance with the Assignment Agreement Letter Implementation of the 2020 Research Program Number: B/87/E3/RA.00/2020.

Acknowledgment

The author is grateful, and this research is facilitated by the Biomaterials and Drug Delivery System (BiDDS) Research Group and Departement of Pharmacy STIKES 'Aisyiyah Palembang. Thanks to the Phytopharmaceutic Research Center (PRC), Department of Pharmacy, Faculty of Mathematics and Natural Sciences, Universitas Sriwijaya. Thanks to the PT DKSH Indonesia.

- systems (SNEDDS) for curcumin transdermal delivery: an anti-inflammatory exposure. *Drug Development and Industrial Pharmacy* 45(7): 1073–1078. <https://doi.org/10.1080/03639045.2019.1593440>
- Anwer MK, Iqbal M, Aldawsari MF, Alalaiwe A, Ahmed MM, Muharram MM, Ezzeldin E, Mahmoud MA, Imam F, Ali R (2021) Improved antimicrobial activity and oral bioavailability of delafloxacin by

- self-nanoemulsifying drug delivery system (SNEDDS). *Journal of Drug Delivery Science and Technology* 64: e102572. <https://doi.org/10.1016/j.jddst.2021.102572>
- Balakumar K, Raghavan CV, Selvan NT, Prasad RH, Abdu S (2013) Self nanoemulsifying drug delivery system (SNEDDS) of rosuvastatin calcium: design, formulation, bioavailability and pharmacokinetic evaluation. *Colloids and Surface B: Biointerfaces* 112: 337–43. <https://doi.org/10.1016/j.colsurfb.2013.08.025>
- Cai Y, Liu L, Xia M, Tian C, Wu W, Dong B, Chu, X (2022) SEDDS facilitate cinnamaldehyde crossing the mucus barrier: the perspective of mucus and Caco-2/HT29 co-culture models. *International Journal of Pharmaceutics* 614: e121461. <https://doi.org/10.1016/j.ijpharm.2022.121461>
- Cardona MI, Dominguez GP, Echeverry SM, Valderrama IH, Bernkop-Schnürch A, Aragón M (2021) Enhanced oral bioavailability of rutin by a self-emulsifying drug delivery system of an extract of calyces from *Physalis peruviana*. *Journal of Drug Delivery Science and Technology* 66: e102797. <https://doi.org/10.1016/j.jddst.2021.102797>
- Cheng SC, Wu YH, Huang WC, Pang JS, Huang TH, Cheng CY (2019) Anti-inflammatory property of quercetin through downregulation of ICAM-1 and MMP-9 in TNF- α -activated retinal pigment epithelial cells. *Cytokine* 116: 48–60. <https://doi.org/10.1016/j.cyto.2019.01.001>
- Cui F, Kim M, Park C, Kim D, Mo K, Kim M (2021) Application of principal component analysis (PCA) to the assessment of parameter correlations in the partial-nitrification process using aerobic granular sludge. *Journal of Environmental Management* 288: e112408. <https://doi.org/10.1016/j.jenvman.2021.112408>
- Dhritlahre RK, Ruchika, Padwad Y, Saneja A (2021) Self-emulsifying formulations to augment therapeutic efficacy of nutraceuticals: From concepts to clinic. *Trends in Food Science & Technology* 115: 347–365. <https://doi.org/10.1016/j.tifs.2021.06.046>
- Dwi S, Febrianti S, Zainul A, Retno S (2018) PEG 8000 increases solubility and dissolution rate of quercetin in solid dispersion system. *Marmara Pharmaceutical Journal* 22(2): 259–266. <https://doi.org/10.12991/npj.2018.63>
- Ferreira CGT, Campos MG, Felix DM, Santos MR, Carvalho OV, Diaz MAN, Fietto JLR, Bressan GC, Silva-Junior A, Almeida MR (2018) Evaluation of the antiviral activities of *Bacharis dracunculifolia* and quercetin on Equid herpesvirus 1 in a murine model. *Research in Veterinary Science* 120: 70–77. <https://doi.org/10.1016/j.rvsc.2018.09.001>
- García del Moral LF, Morgado A, Esquivel JA (2021) Reflectance spectroscopy in combination with cluster analysis as tools for identifying the provenance of Neolithic flint artefacts. *Journal of Archaeological Science Reports* 37: e103041. <https://doi.org/10.1016/j.jasrep.2021.103041>
- Halder S, Islam A, Muhit MA, Shill MC, Haider SS (2021) Self-emulsifying drug delivery system of black seed oil with improved hypotriglyceridemic effect and enhanced hepatoprotective function. *Journal of Functional Foods* 78: e104391. <https://doi.org/10.1016/j.jff.2021.104391>
- Hong Y, Liao X, Chen Z (2020) Determination of bioactive components in the fruits of *Cercis chinensis* Bunge by HPLC-MS/MS and quality evaluation by principal components and hierarchical cluster analysis. *Journal of Pharmaceutical Analysis* 11(4): 465–471. <https://doi.org/10.1016/j.jpha.2020.07.010>
- Iaboni DSM, Farrell SR, Chauhan BC (2020) Morphological multivariate cluster analysis of murine retinal ganglion cells selectively expressing yellow fluorescent protein. *Experimental Eye Research* 196: e108044. <https://doi.org/10.1016/j.exer.2020.108044>
- Indrati O, Martien R, Rohman A, Nugroho AK (2020) Application of simplex lattice design on the optimization of andrographolide self nanoemulsifying drug delivery system (SNEDDS). *Indonesian Journal of Pharmacy* 13(2): 124–130. <https://doi.org/10.14499/indonesianjpharm31iss2pp124>
- Jumaryatno P, Chabib L, Hayati F, Awaluddin R (2018) Stability study of *Ipomoea reptans* extract self-nanoemulsifying drug delivery system (SNEDDS) as anti-diabetic therapy. *Journal of Applied Pharmaceutical Science* 8(9): 11–14. <https://doi.org/10.7324/JAPS.2021.110313>
- Kartini K, Putri LAD, Hadiyat MA (2020) FTIR-based fingerprinting and discriminant analysis of *Apium graveolens* from different locations. *Journal of Applied Pharmaceutical Science* 10(12): 62–67. <https://doi.org/10.7324/JAPS.2020.101208>
- Kim M, Chang JW, Park K, Yang DR (2022) Comprehensive assessment of the effects of operating conditions on membrane intrinsic parameters of forward osmosis (FO) based on principal component analysis (PCA). *Journal of Membrane Science* 641: e119909. <https://doi.org/10.1016/j.memsci.2021.119909>
- Li X, Zhou N, Wang J, Liu Z, Wang X, Zhang Q, Liu Q, Gao L, Wang R (2018) Quercetin suppresses breast cancer stem cells (CD44(+)/CD24(-)) by inhibiting the PI3K/Akt/mTOR-signaling pathway. *Life Sciences* 196: 56–62. <https://doi.org/10.1016/j.lfs.2018.01.014>
- Ogino M, Nakazawa A, Shiokawa K, Kikuchi H, Sato H, Onoue S (2021) Krill oil-based self-emulsifying drug delivery system to improve oral absorption and renoprotective function of ginger extract. *Pharmaceutical Nutrition* 19: e100285. <https://doi.org/10.1016/j.phanu.2021.100285>
- Pratiwi G, Murwanti R, Martien R (2019) Chitosan nanoparticle as a delivery system for polyphenols from meniran extract (*Phyllanthus niruri* L.): Formulation, optimization, and immunomodulatory activity. *International Journal of Applied Pharmaceutics* 11(2): 50–58. <https://doi.org/10.22159/ijap.2019v11i2.29999>
- Pratiwi G, Susanti S, Shiyan S (2020) Application of factorial design for optimization of PVC-HPMC polymers in matrix film ibuprofen patch-transdermal drug delivery system. *Indonesian Journal of Chemometrics and Pharmaceutical Analysis* 1(1): 11–22. <https://doi.org/10.22146/ijcpa.486>
- Puppala RK, Lakshmi VA (2019) Optimization and solubilization study of nanoemulsion budesonide and constructing pseudoternary phase diagram. *Asian Journal of Pharmaceutical and Clinical Research* 12(1): 551–553. <https://doi.org/10.22159/ajpcr.2019.v12i1.28686>
- Setyawan EI, Rohman A, Setyowati EP, Nugroho AK (2021) The combination of simplex lattice design and chemometrics in the formulation of green tea leaves as transdermal matrix patch. *Pharmacia* 68(1): 275–282. <https://doi.org/10.3897/pharmacia.68.e61734>
- Shiyan S, Arifin A, Amriani A, Pratiwi G (2020) Immunostimulatory activity of ethanol extract from *Calotropis gigantea* L. flower in rats against *Salmonella typhimurium* infection. *Research Journal of Pharmacy and Technology* 13(11): 5244–5250.
- Shiyan S, Hertiani T, Martien R, Nugroho AK (2019) Optimization and validation of RP-HPLC/UV detection for several compounds simultaneously in semi-purified extract of white tea. *Rasayan Journal of Chemistry* 12(3): 1098–1109. <https://doi.org/10.31788/RJC.2019.1235276>
- Shiyan S, Suryani RP, Mulyani LN, Pratiwi G (2022) Stability study of super saturable catechin-self nano emulsifying drug delivery system

- as antidiabetic therapy. *Biointerface Research in Applied Chemistry* 12(5): 5811–5820. <https://doi.org/10.33263/BRIAC125.58115820>
- Shiyan S, Zubaidah, Pratiwi G (2021) Chemometric approach to assess response correlation and its classification in simplex centroid design for pre-optimization stage of catechin-SNEDDS. *Research Journal of Pharmacy and Technology* 14(11): 5863–5870. <https://doi.org/10.52711/0974-360X.2021.01020>
- Srinivasan P, Vijayakumar S, Kothandaraman S, Palani M (2018) Anti-diabetic activity of quercetin extracted from *Phyllanthus emblica* L. fruit: In silico and in vivo approaches. *Journal of Pharmaceutical Analysis* 8(2): 109–118. <https://doi.org/10.1016/j.jpha.2017.10.005>
- Szentmiklóssy M, Török K, Pusztai É, Kemény S, Tremmel-Bede K, Rakszegi M, Tömösközi S (2020) Variability and cluster analysis of arabinoxylan content and its molecular profile in crossed wheat lines. *Journal of Cereal Science* 95: e103074. <https://doi.org/10.1016/j.jcs.2020.103074>
- Talekar SD, Haware RV, Dave RH (2019) Evaluation of self-nanoemulsifying drug delivery systems using multivariate methods to optimize permeability of captopril oral films. *European Journal of Pharmaceutical Sciences* 130: 215–224. <https://doi.org/10.1016/j.ejps.2019.01.039>
- Tang SM, Deng XT, Zhou J, Li QP, Ge XX, Miao L (2020) Pharmacological basis and new insights of quercetin action in respect to its anti-cancer effects. *Biomedicine and Pharmacotherapy* 121: e109604. <https://doi.org/10.1016/j.biopha.2019.109604>
- Yadav P, Yadav E, Verma A, Amin S (2014) In vitro characterization and pharmacodynamic evaluation of furosemide loaded self nano emulsifying drug delivery systems (SNEDDS). *Journal of Pharmaceutical Investigation* 44(6): 443–453. <https://doi.org/10.1007/s40005-014-0138-z>
- Zhang N, Zhang F, Xu S, Yun K, Wu W, Pan W (2020) Formulation and evaluation of luteolin supersaturatable self-nanoemulsifying drug. *Journal of Drug Delivery Science and Technology* 58: e101783. <https://doi.org/10.1016/j.jddst.2020.101783>